Università degli studi di Padova
Dipartimento di Fisica e Astronomia

Tesi di Dottorato

Search for heavy resonances decaying into a Z boson and a vector boson in the $\nu\bar{\nu}\ q\bar{q}$ final state at CMS

Supervisor: Prof. Franco Simonetto
Candidate: Lisa Benato

Scuola di Dottorato di Ricerca, XXX ciclo

"I have no special talent. I am only passionately curious."
(A. Einstein)

Contents

Abstract

Chapter 1

Introduction

This analysis searches for signal of heavy resonances decaying into a pair of heavy vector bosons. One Z boson is identified through its invisible decay ($\nu\nu$), while the other is required to decay hadronically into a pair of quarks. The final states probed by this analysis therefore consists in two quarks and two neutrinos, reconstructed as missing transverse energy (met). The hadronically decaying boson (Z, W) is reconstructed as a fat jet, whose mass is used to define the signal region. Two purity categories are exploited, based on the n-subjettines of the fat jet.

The search is performed by examining the distribution of the diboson reconstructed transverse mass of the resonance VZ (mtVZ) for a localized excess. The shape and normalization of the main background of the analysis (V+jets) are estimated with an hybrid approach using the distribution of data in the sidebands, corrected for a function accounting for potential differences between the signal region and the sidebands, while the minor background sources are taken from simulations.

Chapter 2

Theoretical motivation

The standard model (SM) of particles represents, so far, the best available description of the particles and their interactions. It is the summation of two gauge theories: the electroweak interaction, that portrays the weak and electromagnetic interactions together, and the strong interaction, or Quantum Chromodynamics (QCD). Particles, namely quarks and leptons, are described as spin 1/2 fermions, whilst interactions are represented by spin 1 bosons. The symmetry group of the standard model is:

$$SU_C(3) \times SU_L(2) \times U_Y(1), \tag{2.1}$$

where the first factor is related to strong interactions, whose mediators are eight gluons, while $SU_L(2) \times U_Y(1)$ is the electroweak simmetry group, whose mediators are photons and Z-$W^{\pm}$ bosons.
In renormalizable theories, with no anomalies, all gauge bosons are expected to be massless, in contrast with our experimental knowledge. This inconsistency is solved by introducing a new scalar particle, the Higgs boson, that can give mass to weak bosons and fermions via the spontaneous symmetry breaking mechanism.

In the last decades, Standard Model has been accurately probed by many experimental facilities (LEP, Tevatron. LHC), and the results lead to an impressive agreement between theoretical predictions and experiments. The discovery of the Higgs boson at the CERN Large Hadron Collider, measured by both CMS and ATLAS collaborations [1–7], represents not only an extraordinary confirmation of the model, but also the latest biggest achievement in particle physics as a whole.

2.1 Beyond Standard Model theories

Even though the Standard Model is the most complete picture of the universe of the particles, many questions are still left open. From a phenomenological point of view, some experimental observations are not included in the theory:

- in SM, neutrinos are massless (whilst experimentally their masses are confirmed to be non-zero, i.e. by the neutrino oscillations);

- no candidates for dark matter are predicted;
- no one of the fields included in the SM can explain the cosmological inflation;
- SM can not justify the matter-antimatter asymmetry.

From a purely theoretical perspective, some issues are still relevant in the formulation of the model:

- *Flavour problem.*
  The Standard Model has 18 free parameters: 9 fermionic masses; 3 angular parameters in Cabibbo-Kobayashi-Maskawa matrix, plus 1 phase parameter; electromagnetic coupling α; strong coupling α_{strong}; weak coupling α_{weak}; Z mass; the mass of the Higgs boson. Such a huge number of degrees of freedom marks the SM as weakly predictive in the flavour sector.

- *Unification.*
  There is not a "complete" unification of strong, weak and electromagnetic interactions, since each one has its own coupling constant, behaving differently at different energy scales; not to mention the fact that gravitational interaction is completely excluded from the SM.

- *Hierarchy problem.*
  From Quantum Field Theory, it is known that perturbative corrections to the mass of the scalar bosons included in the theory tend to make it increase towards the energy scale at which the considered theory still holds [8]. If the Standard Model is seen as a low-mass approximation of a more general theory valid up to the Planck mass scale (*i.e.*, $\sim 1.2 \times 10^{19}$ GeV), a fine-tuning cancellation of the order of 1 over 10^{34} is needed in order to protect the Higgs mass at the electroweak scale (~ 100 GeV). Such an astonishing correction is perceived as very unnatural.

Numerous Beyond Standard Model theories (BSM) have been proposed in order to overcome the limits of the Standard Model.
Grand Unified Theories (GUT) aim at extending the symmetry group of the SM (eq. 1) into largest candidates, such as $S0(10)$, $SU(5)$ and $E(6)$. At GUT scale, approximately at 10^{16} GeV, non-gravitational interactions are expected to be ruled by only one coupling constant, α_{GUT}.
Super Symmetryc (SUSY) models state that every fermion (boson) of the Standard Model has a bosonic (fermionic) superpartner, with exactly the same quantum numbers, except the spin. If SUSY is not broken, each couple of partners and superpartners should have the same masses, hypothesis excluded by the non-observation of the s-electron. Super Symmetry represents a very elegant solution of the hierarchy problem of the Higgs boson mass, since the perturbative corrections brought by new SUSY particles exactly cancel out the divergences caused by SM particles corrections. A particular sub-class of SUSY models, Minimal Super Symmetric Standard Models, is characterized by the introduction of a new symmetry, the R-parity, that guarantees the proton stability and also the stability of the lightest SUSY particle, a possible good candidate for dark matter.

Two other possible theoretical pictures are extensively described in sec. 2.2-2.3.

2.2 Heavy Vector Triplet

The heavy vector triplet model [9] provides a general framework aimed at studying new physics beyond the standard model, that can manifest into the appearance of new resonances. The adopted approach is that of the simplified model, in which an effective Lagrangian is introduced, in order to describe the properties and interactions of new particles (in this case, a triplet of spin-1 bosons) by using a limited set of parameters, that can be easily linked to the physical observables at the LHC experiments. These parameters can describe many physical motivated theories (such as sequential extensions of the SM [10, 11] or Composite Higgs [12, 13]).
Since a simplified model is not a complete theory, its validity is restricted to the on-shell quantities related to the production and decay mechanisms of the new resonances, that is how most of the LHC BSM searches are performed. Given these conditions, experimental results in the resonant region are sensitive to a limited number of the phenomenological Lagrangian parameters (or to a combination of those), whilst the remaining parameters tend to influence the tail of the distributions.
Limits on production cross-section times branching ratio ($\sigma\mathcal{B}$), as a function of the invariant mass spectrum of the probed resonance, can be extracted from experimental data. Given that $\sigma\mathcal{B}$ are functions of the simplified model parameters and of the parton luminosities, it is then possible to interpret the observed limits in the parameter space.

2.2.1 Simplified Lagrangian

The heavy vector triplet framework assumes the existence of an additional vector triplet, V_μ^a, $a = 1, 2, 3$, in which two spin-1 particles are charged and one is neutral:

$$\begin{aligned} V_\mu^\pm &= \frac{V_\mu^1 \mp i V_\mu^2}{\sqrt{2}}; \\ V_\mu^0 &= V_\mu^3. \end{aligned} \tag{2.2}$$

The triplet interactions are described by a simplified Lagrangian, that is invariant under SM gauge and CP symmetry, and accidentally invariant under the custodial symmetry $SU(2)_L \times SU(2)_R$:

$$\begin{aligned} \mathcal{L}_\mathcal{V} = & -\frac{1}{4}\left(D_\mu V_\nu^a - D_\nu V_\mu^a\right)\left(D^\mu V^{\nu\ a} - D^\nu V^{\mu\ a}\right) + \frac{m_V^2}{2} V_\mu^a V^{\mu\ a} \\ & + i g_V c_H V_\mu^a \left(H^\dagger \tau^a D^\mu H - D^\mu H^\dagger \tau^a H\right) + \frac{g^2}{g_V} c_F V_\mu^a \sum_f \bar{f}_L \gamma^\mu \tau^a f_L \\ & + \frac{g_V}{2} c_{VVV} \epsilon_{abc} V_\mu^a V_\nu^b \left(D^\mu V^{\nu\ c} - D^\nu V^{\mu\ c}\right) + g_V^2 c_{VVHH} V_\mu^a V^{\mu\ a} H^\dagger H - \frac{g}{2} c_{VVW} \epsilon_{abc} W^{\mu\nu\ a} V_\mu^b V_\nu^c. \end{aligned} \tag{2.3}$$

In the first line of the formula 2.3, V mass and kinematic terms are included, described with the covariant derivative $D_\mu V_\nu^a = \partial_\mu V_\nu^a + g \epsilon^{abc} W_\mu^b V_\nu^c$, where W_μ^a are the fields of the weak interaction and g is the weak gauge coupling. V_μ^a are not mass eigenstates, since they mix with the electroweak fields after the spontaneous symmetry breaking, therefore m_V isn't the physical

mass of the V bosons.
The second line describes the interaction of the triplet with the Higgs field and the SM left-handed fermions; c_H describes the vertices with the physical Higgs and the three unphysical Goldstone bosons that, for the Goldstone equivalence theorem, are equivalent to the longitudinal polarization of W and Z bosons at high-energy; hence, c_H is related to the bosonic decays of the resonances. c_F is the analogous parameter describing the V interaction with fermions, that can be generalized as a flavour dependent coefficent, once defined $J_F^{\mu\ a} = \sum_f \bar{f}_L \gamma^\mu \tau^a f_L$: $c_F V_\mu^a J_F^{\mu\ a} = c_\ell V_\mu^a J_\ell^{\mu\ a} + c_q V_\mu^a J_q^{\mu\ a} + c_3 V_\mu^a J_3^{\mu\ a}$.
The last part of the equation includes terms that are relevant only in strongly coupled scenarios (see sec. 2.2.2) through the V-W mixing, but it does not include vertices of V with light SM fields, hence it can be neglected while describing the majority of the LHC phenomenology, under the assumptions previously stated. Additional dimension four quadrilinear V interactions are non relevant for the processes discussed, otherwise their effects would be appreciated in electroweak precision tests and precise Higgs coupling measurements [14].

The parameters in the Lagrangian can be interpreted as follows: g_V describes the strenght of the interaction, that is weighted by c parameters. g_V ranges from $g_V \sim 1$ when the coupling is weak (sec. 2.2.4), to $g_V \sim 4\pi$ when the coupling is strong (sec. 2.2.5). c parameters are expected to be $c \sim 1$, except to c_H, that can be smaller for weak couplings. The combinations describing the vertices, $g_V c_H$ and $g^2/g_v c_F$, can be considered as the fundamental parameters, used to interpret the experimental results.

2.2.2 Mass eigenstates, mixing parameters and decay widths

The newly introduced $SU(2)_L$ triplet is expected to mix with the weak SM fields. The $U(1)_{em}$ symmetry is left unbroken by the new interaction, hence the massless combination of the electroweak fields, namely the photon, is the same as the SM:

$$A_\mu = B_\mu \cos\theta_W + W_\mu^3 \sin\theta_W, \tag{2.4}$$

with the usual definitions of the electroweak parameters:

$$\begin{aligned} \tan\theta_W &= \frac{g'}{g} \\ e &= \frac{g g'}{\sqrt{g^2 + g'^2}} \\ g &= e/\sin\theta_w \\ g' &= e/\cos\theta_w. \end{aligned} \tag{2.5}$$

The Z boson, on the other hand, mixes with the neutral component of the triplet, V^0, with a rotation parametrized with the angle θ_N:

$$\begin{pmatrix} \cos\theta_N & \sin\theta_N \\ -\sin\theta_N & \cos\theta_N d \end{pmatrix} \begin{pmatrix} Z \\ V^0 \end{pmatrix}. \tag{2.6}$$

The mass matrix of the rotated system is given by:

$$\mathbb{M}_N^2 = \begin{pmatrix} \hat{m}_Z^2 & c_H \zeta \hat{m}_Z \hat{m}_V \\ c_H \zeta \hat{m}_Z \hat{m}_V & \hat{m}_V^2 \end{pmatrix}, \tag{2.7}$$

where the parameters are defined as:

$$\begin{cases} \hat{m}_Z = \frac{e}{2\sin\theta_W\cos\theta_W}\hat{v} \\ \hat{m}_V^2 = m_V^2 + g_V^2 c_{VVHH}\hat{v}^2 \\ \zeta = \frac{g_V\hat{v}}{2\hat{m}_V} \\ \frac{\hat{v}^2}{2} = \langle H^\dagger H\rangle \end{cases}, \tag{2.8}$$

and $\hat{v}$, the vacuum expectation value of the Higgs field, can be different from the SM $v = 246$ GeV. The physical masses of Z and V^0, m_Z and M_0, and θ_N come from the matrix relations:

$$\begin{aligned} &\mathrm{Tr}\left(\mathbb{M}_N^2\right) = \hat{m}_Z^2 + \hat{m}_V^2 = m_Z^2 + M_0^2 \\ &\left\|\mathbb{M}_N^2\right\| = \hat{m}_Z^2 + \hat{m}_V^2\left(1 - c_H^2\zeta^2\right) = m_Z^2 M_0^2 \\ &\tan 2\theta_N = \frac{2c_H\zeta\hat{m}_Z\hat{m}_V}{\hat{m}_V^2 - \hat{m}_Z^2}. \end{aligned} \tag{2.9}$$

The $W^\pm$ bosons mix with the charged components of the triplet, $V^\pm$, leading to a mass matrix analogous to eq. 2.10:

$$\mathbb{M}_C^2 = \begin{pmatrix} \hat{m}_W^2 & c_H\zeta\hat{m}_W\hat{m}_V \\ c_H\zeta\hat{m}_W\hat{m}_V & \hat{m}_V^2 \end{pmatrix}, \tag{2.10}$$

where $\hat{m}_W$ is defined as:

$$\left\{\ \hat{m}_W = \frac{e}{2\sin\theta_W}\hat{v} = \hat{m}_Z\cos\theta_W\ ; \right. \tag{2.11}$$

the physical masses of W and $V^\pm$, m_W and $M_\pm$, and the angle θ_C parametrizing the rotation of the charged sector are described by:

$$\begin{aligned} &\mathrm{Tr}\left(\mathbb{M}_C^2\right) = \hat{m}_W^2 + \hat{m}_V^2 = m_W^2 + M_\pm^2 \\ &\left\|\mathbb{M}_C^2\right\| = \hat{m}_W^2 + \hat{m}_V^2\left(1 - c_H^2\zeta^2\right) = m_W^2 M_\pm^2 \\ &\tan 2\theta_C = \frac{2c_H\zeta\hat{m}_W\hat{m}_V}{\hat{m}_V^2 - \hat{m}_W^2}. \end{aligned} \tag{2.12}$$

The custodial symmetry of eq. 2.3 guarantees that:

$$\mathbb{M}_C^2 = \begin{pmatrix} \cos\theta_W & 0 \\ 0 & 1 \end{pmatrix}\mathbb{M}_N^2\begin{pmatrix} \cos\theta_W & 0 \\ 0 & 1 \end{pmatrix}. \tag{2.13}$$

By taking the determinant of these matrices, a custodial relation among the masses can be extracted:

$$m_W^2 M_\pm^2 = \cos\theta_W m_Z^2 M_0^2, \tag{2.14}$$

that has some very important consequences.
Given that this model aims at searching new particles in the TeV scale and that the scale of the electroweak interactions must lay at ~ 100 GeV, a hierarchy of the physical masses seems very natural:

$$\frac{\hat{m}_{(W,Z)}}{\hat{m}_V} \sim \frac{m_{(W,Z)}}{M_{(\pm,0)}} \ll 1; \tag{2.15}$$

ζ parameter can be $\zeta \ll 1$ (weakly coupled scenario) or $\zeta \sim 1$ (strongly coupled scenario). When eq. 2.15 applies, the second lines in eq. 2.9 and eq. 2.12 can be approximated as follows:

$$\begin{array}{l} m_Z^2 = \hat{m}_Z^2 \left(1 - c_H^2 \zeta^2\right) \left(1 + \mathcal{O}(\hat{m}_Z^2 / \hat{m}_V^2)\right) \\ m_W^2 = \hat{m}_W^2 \left(1 - c_H^2 \zeta^2\right) \left(1 + \mathcal{O}(\hat{m}_W^2 / \hat{m}_V^2)\right) \end{array}. \tag{2.16}$$

From eq. 2.11, the ratio of the physical masses of the charged and neutral electroweak bosons can be approximated as:

$$\frac{m_W^2}{m_Z^2} \approx \cos\theta_W{}^2, \tag{2.17}$$

that satisfies the SM tree-level relation $\rho = 1$ if $\cos\theta_W{}^2 \approx 1. - 0.23$. Adding this approximation into eq. 2.14, the V bosons are expected to have the same masses, hence the same production rates:

$$M_\pm^2 = M_0^2 \left(1 + \mathcal{O}(\%)\right). \tag{2.18}$$

The degenerate mass of the triplet will be called $M_V \approx M_\pm \approx M_0$; given 2.15, $M_V = \hat{m}_V$. Another consequence of the mass hierarchy (2.15) is that the mixing angles $\theta_{(N,C)}$ between the electroweak fields and the triplet are small:

$$\theta_{(N,C)} \approx c_H \zeta \frac{\hat{m}_{(W,Z)}}{\hat{m}_V} \ll 1, \tag{2.19}$$

hence the couplings among SM particles are very close to the couplings predicted by the SM.

Decay widths into fermions

The couplings among the triplet and SM fermions are expressed as a function of the rotation angles $\theta_{(C,N)}$ and SM couplings (omitting the CKM matrix elements for quarks):

$$\begin{array}{l} \left\{ \begin{array}{l} g_L^N = \frac{g^2}{g_V} \frac{c_F}{2} \cos\theta_N + \left(g_L^Z\right)_{SM} \sin\theta_N \approx \frac{g^2}{g_V} \frac{c_F}{2} \\ g_R^N = \left(g_R^Z\right)_{SM} \sin\theta_N \approx 0 \end{array} \right. , \\ \left\{ \begin{array}{l} g_L^C = \frac{g^2}{g_V} \frac{c_F}{2} \cos\theta_C + \left(g_L^W\right)_{SM} \sin\theta_N \approx \frac{g^2}{g_V} \frac{c_F}{2} \\ g_R^C = 0 \end{array} \right. , \end{array} \tag{2.20}$$

where $g_L^W = g/\sqrt{2}$; $g_{L,R}^{W,Z}$ are those predicted by the standard model. The V bosons interact with SM left fermions, and the strenght of the couplings with fermions is determined by $g^2/g_V c_F$, as stated in sec. 2.2.1. The decay width into fermions is then given by:

$$\Gamma_{V^\pm \to f\bar{f}'} \approx 2\Gamma_{V^0 \to f\bar{f}} \approx N_c \left(\frac{g^2 c_F}{g_V}\right)^2 \frac{M_V}{48\pi}, \tag{2.21}$$

where N_c is the number of colours (3 for quarks, 1 for leptons).

Decay widths into bosons

As a starting point, a proper choice of the gauge makes the derivation of the approximate decay widths easier. While the unitary gauge is very convenient in discussing the electroweak symmetry breaking mechanism, since it provides a basis in which the Goldstone components of the scalar fields of the theory are set to zero, it does not properly describe the logitudinally polarized bosons in high-enery regimes, since it introduces a dependence of the type E/m in the logitudinal polarization vector, not corresponding to the experimental results. This pathological behaviour can be overcome profiting of the equivalence theorem: while calculating the scattering amplitude of an high-energy process, the longitudinally polarized vectors are equivalent to their corresponding Goldstone scalars. The scattering amplitude can therefore be calculated with Goldstone diagrams.
In the so-called equivalent gauge [15], the Higgs doublet is then parametrized as:

$$H = \begin{pmatrix} i\pi_+ \\ \frac{\hat{h}+h-i\pi_0}{\sqrt{2}} \end{pmatrix}, \tag{2.22}$$

and the Goldstones π_0 and π_+ describe respectively W and Z longitudinal bosons; h is the physical Higgs boson. Rewriting the simplified Lagrangian 2.3 with 2.22 parametrization, two terms hold the information of the interaction of the Vs with the Goldstones:

$$\mathcal{L}_\pi = ... + c_H \zeta \hat{m}_V V_\mu^a \partial^\mu \pi^a + \frac{g_V c_H}{2} V_\mu^a \left(\partial^\mu h \pi^a - h \partial^\mu \pi^a + \epsilon^{abc} \pi^b \partial^\mu \pi^c \right) + ..., \tag{2.23}$$

that are ruled by the $c_H g_V$ parameters combination. When ζ parameter is $\zeta \approx 1$, the first term in eq. 2.23 becomes important, and it is absorbed by a redefinition of the V_μ^a and π^a fields,

$$\begin{aligned} V_\mu^a &\to V_\mu^a + \frac{c_H \zeta}{\hat{m}_V} \partial_\mu \pi^a \\ \pi^a &\to \frac{1}{\sqrt{1 - c_H^2 \zeta^2}} \pi^a; \; c_H^2 \zeta^2 < 1 \end{aligned}. \tag{2.24}$$

By properly taking into account all the terms of the simplified lagrangian in the equivalent gauge, the partial widths of the dibosonic decays are ($\hat{m}_V = M_V$):

$$\begin{aligned} \Gamma_{V^0 \to W_L^+ W_L^-} \approx \Gamma_{V^\pm \to W_L^\pm Z_L} &\approx \frac{g_V^2 c_H^2 M_V}{192\pi} \frac{\left(1 + c_H c_{VVV} \zeta^2\right)^2}{\left(1 - c_H^2 \zeta^2\right)^2} = \frac{g_V^2 c_H^2 M_V}{192\pi} \left(1 + \mathcal{O}(\zeta^2)\right) \\ \Gamma_{V^0 \to Z_L h} \approx \Gamma_{V^\pm \to W_L^\pm h} &\approx \frac{g_V^2 c_H^2 M_V}{192\pi} \frac{\left(1 - 4 c_H c_{VVV} \zeta^2\right)^2}{\left(1 - c_H^2 \zeta^2\right)^2} = \frac{g_V^2 c_H^2 M_V}{192\pi} \left(1 + \mathcal{O}(\zeta^2)\right). \end{aligned} \tag{2.25}$$

Decays in fermions and bosons: concluding remarks

From eq. 2.21-2.25, some important conclusions can be extracted.

- When ζ parameter is small, all the triplet decays (both in fermions and in dibosons), branching fractions and productions are completely determined by $g^2 c_F / g_V$, $g_V c_H$, and the degenerate mass of the triplet M_V,
- c_{VVV}, c_{VVHH}, c_{VVW} can be neglected, as long as the interest is focused in narrow resonances.

2.2.3 HVT production

Given the mass scale of the resonances, the production mechanisms expected to be relevant are Drell-Yan (fig. 2.1) and Vector Boson Fusion (VBF) (fig. 2.2).

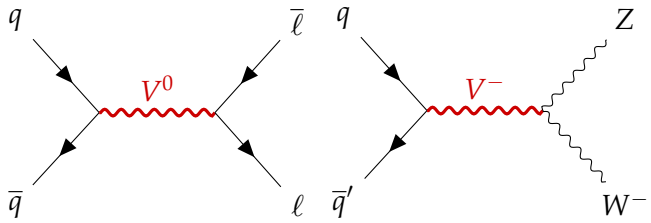

Figure 2.1: Examples of Drell-Yan production mechanism of a heavy V HVT boson: $q - \bar{q}$ quark scattering producing a neutral V^0 that decays leptonically (left); $q - \bar{q}'$ scattering producing a charged V^- that decays in a W and Z bosons (right).

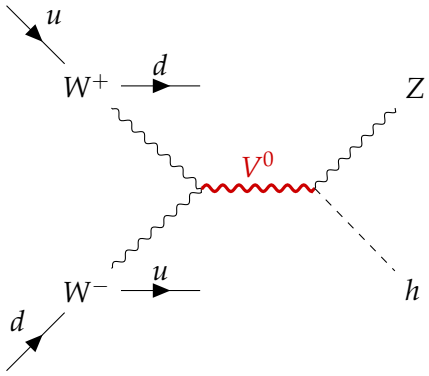

Figure 2.2: Example of VBF production mechanism of a heavy V HVT boson: a neutral V^0 boson is produced by a couple of W bosons, as a result of electroweak interactions of initial state u and d quarks. V^0 decays in a Z boson and a Higgs boson. The final state signature includes the presence of a pair of quarks, due to the primary interactions.

The cross-section of the production mechanisms is given by:

$$\sigma(pp \to V + X) = \sum_{i,j \in p} \frac{\Gamma_{V \to ij}}{M_V} f(J, S_i, S_j) g(C_i, C_j) \frac{dL_{ij}}{ds}\bigg|_{s=M_V^2}, \tag{2.26}$$

where i, j are the partons involved in the hard interaction, Γ_{ij} is the partial width of the process $V \to ij$, $f(J, S_i, S_j)$ is a function of the spin of the resonance and of the partons, $g(C_i, C_j)$ is a function of the colour factors of each parton, s is the center-of-mass energy and $\frac{dL_{ij}}{ds}$ are the parton luminosities, that are independent from HVT model (that enters only in Γ_{ij}).
Parton luminosities, calculated for a center-of-mass energy of 14 TeV starting from quark and antiquark parton distribution functions (PDF), are displayed in fig. 2.3 (Drell-Yan mechanism) and 2.4 (VBF mechanism). VBF luminosities are suppressed by the α_{EW} factor, therefore the process is relevant only when the bosonic decays of the triplet are dominant (strongly coupled scenario).

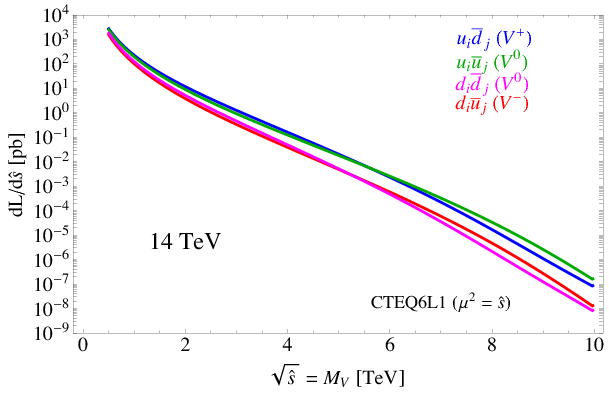

Figure 2.3: Parton luminosities for Drell-Yan process between i and j partons, as a function of the parton center-of-mass energy, for the LHC proton-proton collisions performed at 14 TeV.

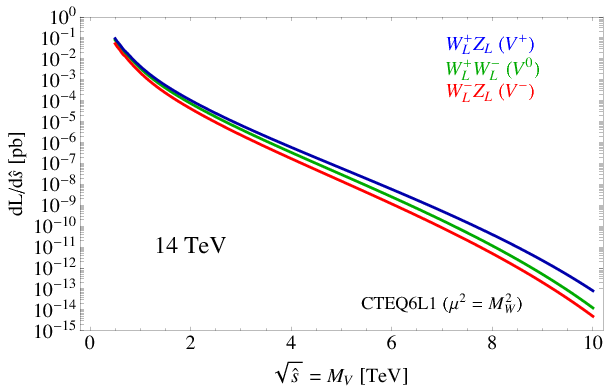

Figure 2.4: Parton luminosities for VBF process between i and j partons, as a function of the parton center-of-mass energy, for the LHC proton-proton collisions performed at 14 TeV.

2.2.4 Benchmark model A: weak coupling scenario

Model A scenario aims at reproducing a simple generalization of the SM [10], obtained by extending the gauge symmetry group with an additional $SU(2)'$. The low-energy phenonemna are expected to be dominated by the SM, while the high-energy processes are relevant for the additional symmetry, bringing additional light vector bosons in play.
It can be shown that this kind of picture is portrayed by HVT when $c_H \sim -g^2/g_V^2$ and $c_F \sim 1$. This implies that:

$$\begin{aligned} g_V c_H &\approx g^2/g_V \\ g^2 c_F/g_V &\approx g^2/g_V, \end{aligned} \tag{2.27}$$

hence the partial decay widths into fermions (eq. 2.21) and bosons (eq. 2.25) differ only by a factor 2 and the colour factor (N_c). Branching fractions for the model A benchmark scenario ($g_V = 1$) are shown in fig. 2.5 (left); total widths are reported in fig.2.5 (right) for different coupling parameters g_V.

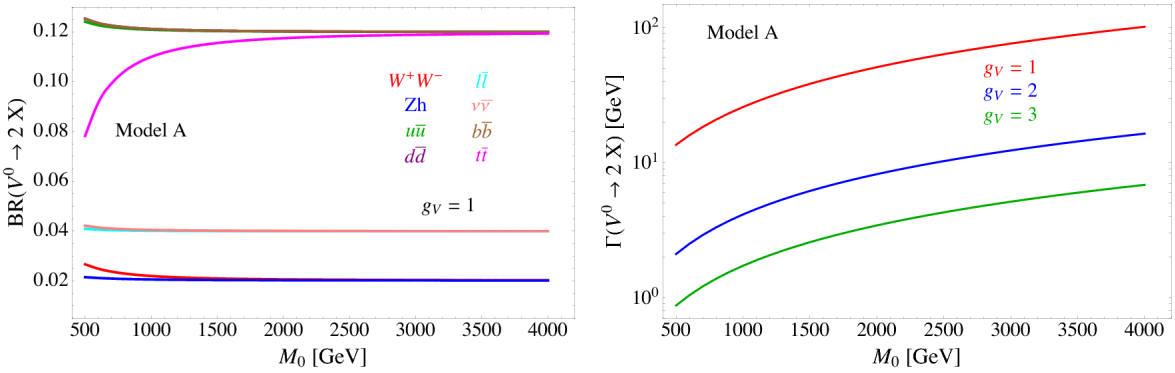

Figure 2.5: HVT model A scenario: branching fractions for fermionic and bosonic decays when $g_V = 1$ (left) as a function of the mass of the resonance M_0; total width of the resonance, as a function of its mass, considering different values of the parameter g_V (right).

2.2.5 Benchmark model B: strong coupling scenario

In composite Higgs models [12], the Higgs boson is the result of the spontaneous symmetry breaking of an $SO(5)$ symmetry to a $SO(4)$ group. New vector bosons are expected to appear, and the lightest ones can be represented by HVT model B when $c_H \sim c_F \sim 1$.
In this case:

$$\begin{aligned} g_V c_H &\approx -g_V \\ g^2 c_F / g_V &\approx g^2 / g_V, \end{aligned} \tag{2.28}$$

hence the decay into bosons is not suppressed by g_V parameter. In the benchmark scenario $g_V = 3$, decays into dibosons are largely dominant, as it can be seen in fig. 2.6 (left); the total decay width increases for larger g_V (fig. 2.6, right). When the resonances start to be very broad, *i.e.* $\Gamma/M_V \gg 0.1$, the assumptions leading to the simplified model are no longer valid, hence higher order, non-resonant effects must be taken into account.

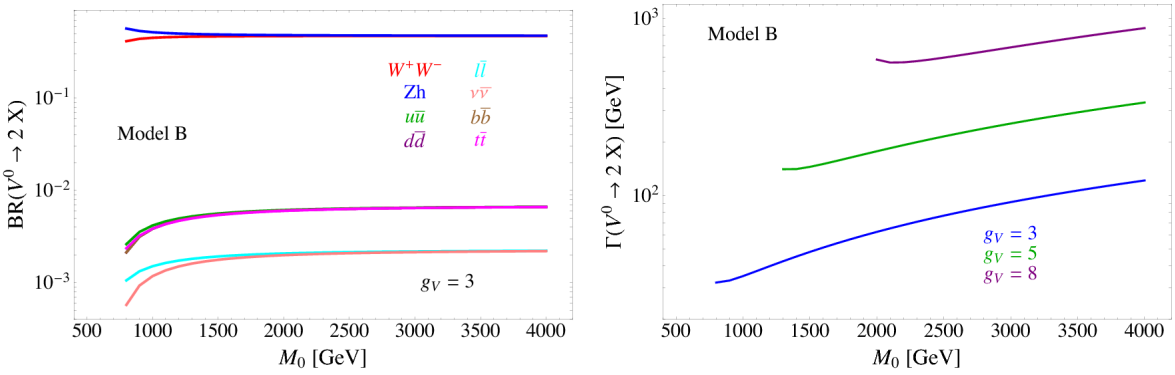

Figure 2.6: HVT model B scenario: branching fractions for fermionic and bosonic decays when $g_V = 3$ (left) as a function of the mass of the resonance M_0; total width of the resonance, as a function of its mass, considering different values of the parameter g_V (right).

2.2.6 Search for HVT resonances at LHC

No evidence of HVT resonances has been observed so far at LHC experiments. Data collected by ATLAS and CMS detectors are used to set limits on the HVT resonance masses and coupling parameters. Experimental results from proton-proton collisions performed at a center-of-mass energy of 8 TeV (Run 1 era) at LHC brought to the following conclusions. A weakly coupled resonance, in the context of benchmark model A ($g_V = 1$) was excluded up to 3 TeV by Run 1 data. By looking at parton luminosities in fig.2.3, in data produced by LHC proton-proton collision at 14 TeV, collected for an integrated luminosity of 300 fb^{-1}, the sensitivity is expected to increase up to $m_V \approx 6$ TeV. A strongly coupled resonance, in the context of benchmark model B ($g_V = 3$) is excluded up to 2 TeV by Run 1 data. Data produced by LHC at 14 TeV should increase the sensitivity up to $m_V \approx 3 - 4$ TeV.
The most stringent limits are provided by the latest data produced by LHC at a center-of-mass energy of 13 TeV (Run 2 era).

Numerous searches for HVT triplet have been performed at CMS experiment in different final states: the most sensitive ones were those in all-hadronic topology. [16, 17] (search for WW, WZ, ZZ resonances in the $q\bar{q}q\bar{q}$ final state) excludes a W' with mass below 3.6 and a Z' with mass below 2.7 TeV in the model B scenario (fig. 2.7). [18, 19] (search for WH, ZH resonances in the $q\bar{q}b\bar{b}$ final state) excludes a W' lighter than 2.97 (3.15) TeV in the HVT model A (model B), and a Z' up to 1.67 (2.26) TeV in HVT model A (model B) (fig. 2.8). In fig. 2.9, results of [16,17] (left) and [18,19] (right) searches are interpreted as exclusion contours in the coupling parameter plane of the HVT model ($g_V c_H$ and $g^2 c_F / g_V$). In the grey shaded area, the narrow width approximation fails. The colored curves display the parameter exclusion for different mass hypoteses of the triplet. Colored dots show the model A and B benchmark scenarios.

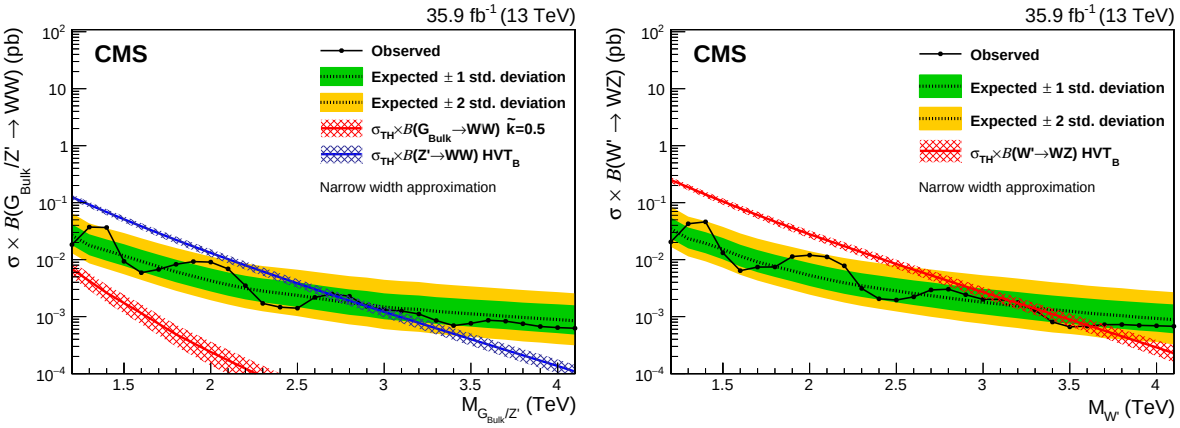

Figure 2.7: The observed and expected limits, with 68% and 95% uncertainty bands, on the product of the cross section and branching fraction $\sigma\mathcal{B}(Z' \to WW)$ for a spin-1 Z' (left) and $\sigma\mathcal{B}(W' \to WZ)$ for a spin-1 W' (right), as a function of the reconstructed mass of the diboson resonance. The colored lines show the theoretical predictions for the HVT model B.

Many other final states have been exploited at CMS: $ZW, ZZ \to \ell\bar{\ell}q\bar{q}$ [20]; $WH, ZH \to (\ell\bar{\ell}, \ell\nu, \nu\bar{\nu})b\bar{b}$ [21]; $WZ, WW \to \ell\nu q\bar{q}$ [22]. Finally, $ZW, ZZ \to \nu\bar{\nu}q\bar{q}$ [23] results will be extensively described in this thesis.

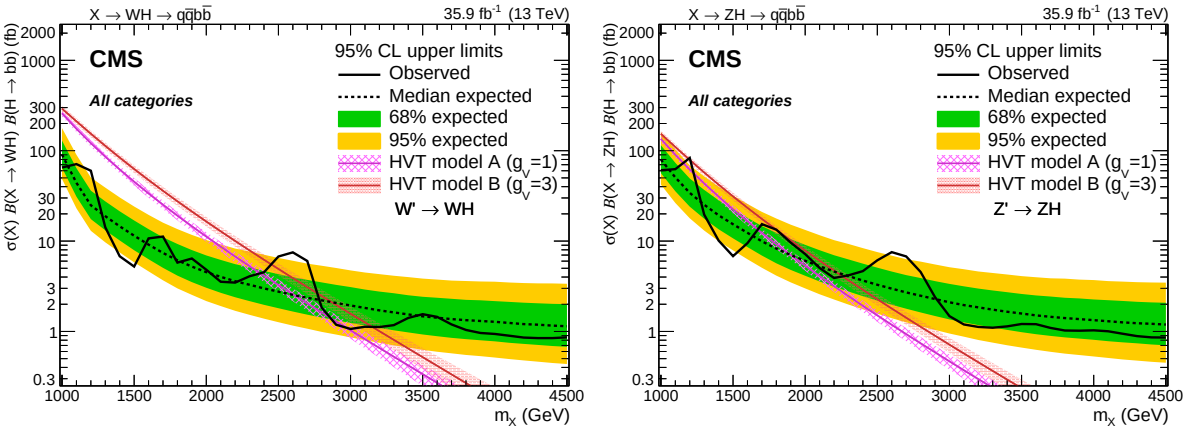

Figure 2.8: The observed and expected limits, with 68% and 95% uncertainty bands, on the product of the cross section and branching fraction $\sigma\mathcal{B}(W' \to WH)$ for a spin-1 W' (left) and $\sigma\mathcal{B}(Z' \to ZH)$ for a spin-1 Z' (right), as a function of the reconstructed mass of the diboson resonance. The colored lines show the theoretical predictions for the HVT model A and B.

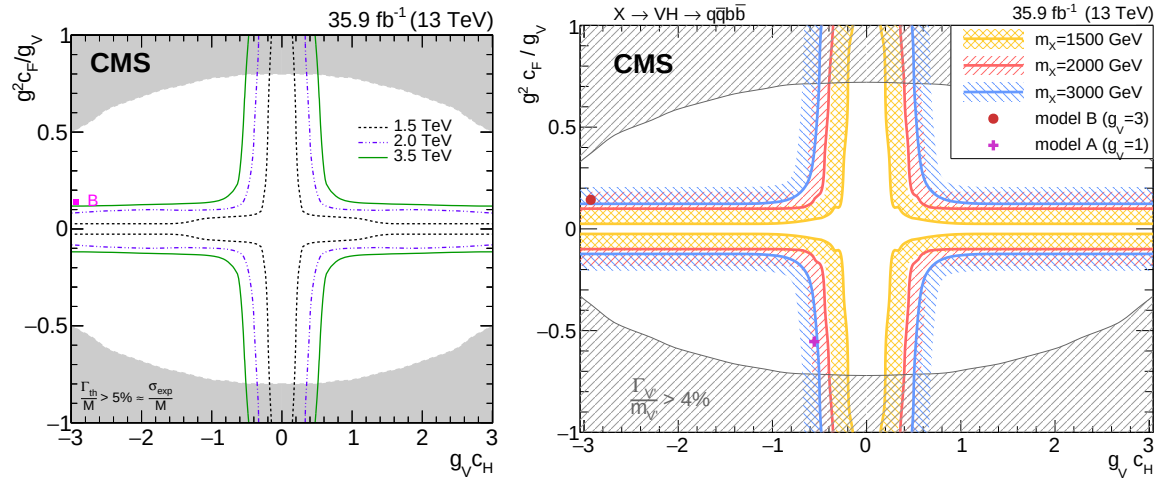

Figure 2.9: Exclusion contours in the coupling parameter plane of the HVT model ($g_V c_H$ and $g^2 c_F / g_V$).

Searches for HVT model B resonances have been performed at ATLAS experiment as well. Results for a $W' \to WZ$ reported in fig. 2.10 include the searches performed in $WW, WZ, ZZ \to q\bar{q}q\bar{q}$ final state [24]; $WZ, WW \to \ell\nu q\bar{q}$ final state [25]; $ZW, ZZ \to (\ell\bar{\ell}, \ell\nu, \nu\bar{\nu})q\bar{q}$ final state [26]. The all-hadronic final state has the best sensitivity and it excludes a W' resonance up to 3.3 TeV (model B scenario). Results for a $W' \to WH$ and for a $Z' \to ZH$ are displayed in fig. 2.11 (left and right respectively), and they include searches performed in $WH, ZH \to q\bar{q}b\bar{b}$ final state [27], and $WH, ZH \to \ell\bar{\ell}, \ell\nu, \nu\bar{\nu})b\bar{b}$ [28]. A W' is excluded up to 2.9 TeV and a Z' is excluded up to 2.8 TeV (in the model B scenario).

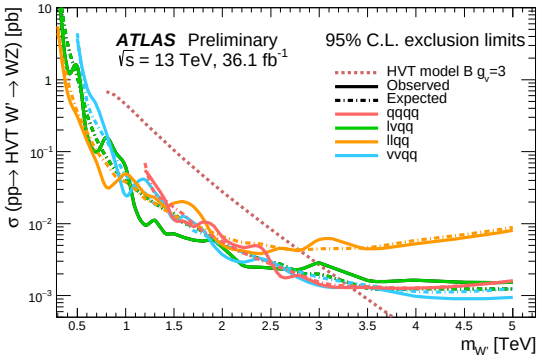

Figure 2.10: The observed and expected limits on the product of the cross section and branching fraction $\sigma\mathcal{B}(W' \to WZ)$ for a spin-1 W', as a function of the reconstructed mass of the diboson resonance. The dotted line shows the theoretical predictions for the HVT model B.

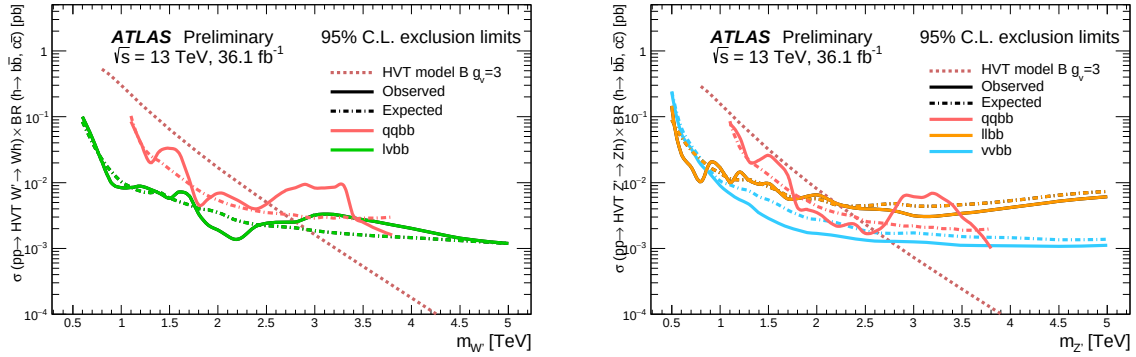

Figure 2.11: The observed and expected limits on the product of the cross section and branching fraction $\sigma\mathcal{B}(W' \to WH)$ for a spin-1 W' (left) and $\sigma\mathcal{B}(Z' \to ZH)$ for a spin-1 Z' (right), as a function of the reconstructed mass of the diboson resonance. The colored lines show the theoretical predictions for the HVT model B.

2.3 Warped extra dimension

The Randall-Sundrum model [29,30] (RS1) proposes the introduction of one additional warped dimension in order to solve the hierarchy problem. The metric of the 5-dimensional space (a slice of AdS_5) generates an exponential hierarchy between the electroweak and Planck scales, associated respectively to the TeV three-brane, where the SM particles are confined, and the Planck three-brane. As a consequence of the new geometry, spin-2 massive gravitons are predicted to exist.
The bulk extension of the Randall-Sundrum model [31,32] states that the SM fields can propagate in the extra dimension. Light fermions are near the Planck brane, heavy fermions are close to the TeV brane, while the Higgs sector is confined in the TeV brane. Higgs couplings to the heavy fermions are therefore expected to be stronger: this naturally arising hierarchy of the masses of the SM fields gives a solution to the flavour problem. In this scenario, the fermionic decays of the bulk gravitons are suppressed, while the bosonic decays are preferred.

2.3.1 Randall-Sundrum original model (RS1)

The existence of additional n-dimensions implies that the effective Planck scale observed in 4-dimensions, $M_{PL} = 1.220910^{19}$ GeV, is related to the fundamental 4+n-dimensional Planck scale, M, via the geometry. M is expected to be of the order of the reduced $\overline{M}_{PL} = M_{PL}/2\pi$. If the 4-dimensional and the n additional metrics are factorizable, $\overline{M}_{PL}$ is the product of M and the volume of the compact space V_n:

$$\overline{M}_{PL}^2 = V_n M^{2+n}. \tag{2.29}$$

If $M \sim$ TeV, this implies that V_n must be very large, hence the compactification scale $\mu \sim 1/V_n^{1/n}$ is small (eV – MeV for n=2 – 7). Given the smallness of μ when compared to the electroweak scale, the effects of the extra dimensions should be evident in SM processes. Since they are not observed, SM particles are assumed to be confined in a 4-dimensional space, the TeV three-brane, while only gravity is allowed to propagate into the 4+n-dimensional space, the bulk. This mechanism solves the hierarchy of the Higgs scale but introduces a new hierarchy between μ and M.
In the Randall-Sundrum model [29, 30], only one additional dimension is added. The geometry of the 5-dimensional bulk is non-factorizable, and it is a slice of AdS_5 spacetime.[1] The 4-dimensional metric is multiplied by an exponential function of the fifth dimension (the "warp" factor):

$$ds^2 = e^{-2kr_c\phi}\eta_{\mu\nu}dx^\mu dx^\nu + r_c^2 d\phi^2; \tag{2.30}$$

x^μ are the usual 4-dimensional coordinates, $\eta_{\mu\nu} = diag(-1,1,1,1)$ is the Minkowski metric, k is a scale of order of $\overline{M}_{PL}$, ϕ is the coordinate of the extra dimension, $0 < |\phi| < \pi$, and r_c is the compactification radius of this finite interval. 4-dimensional mass scales are obtained by multiplying the bulk masses by $e^{-2kr_c\phi}$: given the exponential form of the warp factor, a small r_c suffices for generating a large hierarchy between Planck and Higgs scales.
Two 4-dimensional three-branes are located at the boundaries of the fifth dimension: the

[1] An n-dimensional anti-de Sitter space (AdS_n) is a maximally simmetric Lorentiaz mainfold, that solves the Einstein equation with a negative curvature (negative cosmological constant).

visible brane at $\phi = \pi$; the hidden brane at $\phi = 0$, and their metrics are obtained starting from the bulk 5-dimensional metric G_{MN}, where $M, N = \mu, \phi$:

$$\begin{aligned} g^{\text{vis}}_{\mu\nu}(x^\mu) &= G_{\mu\nu}\left(x^\mu, \phi = \pi\right) \\ g^{\text{hid}}_{\mu\nu}(x^\mu) &= G_{\mu\nu}\left(x^\mu, \phi = 0\right). \end{aligned} \tag{2.31}$$

The classical action is given by:

$$\begin{aligned} S &= S_{\text{gravity}} + S_{\text{vis}} + S_{\text{hid}} \\ S_{\text{gravity}} &= \int d^4x \int_{-\pi}^{+\pi} d\phi \sqrt{-G}\left(-\Lambda + 2M^3\mathcal{R}\right) \\ S_{\text{vis}} &= \int d^4x \sqrt{-g_{\text{vis}}}\left(\mathcal{L}_{\text{vis}} - V_{\text{vis}}\right) \\ S_{\text{hid}} &= \int d^4x \sqrt{-g_{\text{hid}}}\left(\mathcal{L}_{\text{hid}} - V_{\text{hid}}\right), \end{aligned} \tag{2.32}$$

where G (g) is the trace of the G_{MN} ($g_{\mu\nu}$) metric, Λ is the cosmological constant in the bulk, $\mathcal{R}$ is the 5-dimensional Ricci scalar, $\mathcal{L}$ and V are the lagrangian and the vacuum energy of the hidden and visible branes.
A 5-dimensional metric that preserves the 4-dimensional Poincaré invariance has the form:

$$ds^2 = e^{-2\sigma(\phi)}\eta_{\mu\nu}dx^\mu dx^\nu + r_c^2 d\phi^2. \tag{2.33}$$

The Poincaré invariance guarantees that r_c does not depend on x^μ. Given 2.33, the solution of the 5-dimensional Einstein's equations simplifies into:

$$\sigma = r_c\,|\phi|\,\sqrt{\frac{-\Lambda}{24M^3}}. \tag{2.34}$$

Furthermore, the Poincaré invariance imposes constraints to the vacuum energies and cosmological constant:

$$\begin{aligned} V_{\text{hid}} &= -V_{\text{vis}} = 24M^3k \\ \Lambda &= -24M^3k^2. \end{aligned} \tag{2.35}$$

The final 5-dimensional metric is then:

$$ds^2 = e^{-2kr_c|\phi|}\eta_{\mu\nu}dx^\mu dx^\nu + r_c^2 d\phi^2. \tag{2.36}$$

A small r_c is considered, so the effects of the fifth dimension on 4-dimensional spacetime can't be appreciated. A 4-dimensional effective field theory approach is therefore motivated, and its mass parameters are related to the bulk parameters, M, k and r_c. In the Randall-Sundrum model, SM matter fields are confined in the TeV brane.
The massless gravitons, the mediators of the gravitaional interaction in the effective field theory, are the zero modes ($h_{\mu\nu}$) of the quantum fluctuations of the classical solution (2.36):

$$ds^2 = e^{-2kT(x)|\phi|}\left(\eta_{\mu\nu} + h_{\mu\nu}(x)\right)dx^\mu dx^\nu + T^2(x)d\phi^2, \tag{2.37}$$

where the usual Minkowski metric has been replaced by $\overline{g}_{\mu\nu}(x) = \eta_{\mu\nu} + h_{\mu\nu}$; $h_{\mu\nu}$ are the tensor fluctuations around the Minkowski space, and represent both the physical graviton in

4-dimensions and the massless mode of the Kaluza-Klein decomposition of the bulk metric. r_c is the vacuum expectation value of $T(x)$.
By substituting eq. 2.37 in the classical action 2.32, an effective action can be extracted, and in particular the curvature term holds:

$$S_{\text{eff}} \sim \int d^4x \int_{-\pi}^{+\pi} d\phi 2M^3 r_c e^{-2kr_c|\phi|} \overline{\mathcal{R}} \sqrt{-\overline{g}}, \tag{2.38}$$

where $\overline{g}$ is the trace of $\overline{g}_{\mu\nu}$ and $\overline{\mathcal{R}}$ is the 4-dimensional Ricci scalar of $\overline{g}_{\mu\nu}$ metric. In this effective 4-dimensional action, the ϕ dependence can be integrated out, and the 4-dimensional Planck mass can be calculated:

$$\overline{M}_{PL}^2 = M^3 r_c \int_{-\pi}^{+\pi} d\phi e^{-2kr_c|\phi|} = \frac{M^3}{k}\left(1 - e^{-2kr_c\pi}\right). \tag{2.39}$$

It can be shown [29] that a field with a fundamental mass parameter m_0 in the bulk manifests in the visible three-brane with a physical mass m:

$$m = e^{-2kr_c\pi} m_0. \tag{2.40}$$

Scales $m \sim$ TeV are generated from $m_0 \sim \overline{M}_{PL}$ if $e^{kr_c\pi} \sim 10^{15}$. This relation stands still when Higgs field is introduced and confined in the visible three-brane:

$$v = e^{-2kr_c\pi} v_0, \tag{2.41}$$

where v is the Higgs vacuum expectation value in the TeV brane and v_0 is the 5-dimensional Higgs v.e.v.
The hierarchy problem is then solved by the exponential warp factor. The weakness of gravity in the TeV three-brane is motivated by the small overlap of the graviton wave function.
In order to calculate the mass specturm of the graviton in the TeV brane, the tensor fluctuations of the Minkowski metric are expanded into a Kaluza-Klein (KK) tower $h_{\mu\nu}^{(n)}$:

$$h_{\mu\nu}(x,\phi) = \sum_{n=0}^{\infty} h_{\mu\nu}^{(n)}(x) \frac{\chi^{(n)}(\phi)}{\sqrt{r_c}}. \tag{2.42}$$

Once a suitable gauge is chosen, *i.e.* $\eta^{\mu\nu}\partial_\mu h_{\nu\alpha}^{(n)} = \eta^{\mu\nu} h_{\mu\nu}^{(n)} = 0$, the equation of motion of $h_{\mu\nu}^{(n)}$ becomes the Klein-Gordon relation, where $m_n^G \geq 0$:

$$\left(\eta^{\mu\nu}\partial_\mu\partial_\nu - (m_n^G)^2\right) h_{\mu\nu}^{(n)}(x) = 0. \tag{2.43}$$

By substituting eq. 2.42 into Einstein's equation, the solutions for $\chi^{(n)}(\phi)$ (commonly called "profiles") are [33,34]:

$$\chi^{(n)}(\phi) = \frac{e^{2\sigma}}{N}\left[J_2(z_n^G) + \alpha_n Y_2(z_n^G)\right], \tag{2.44}$$

where J_2 and Y_2 are second order Bessel functions, N is the normalization of the wavefunction, α_n are coefficients and $z_n^G = m_n^G e^{\sigma(\phi)}/k$. m_n^G is the mass of the n-mode, and it depends on the roots of the Bessel functions $z_n^G = (3.83, 7.02, 10.17, 13.32, ...)$. In the limit $m_n^G/k \ll 1$ and $e^{kr_c\pi} \gg 1$:

$$m_n^G = k z_n^G(\pi) e^{-kr_c\pi}. \tag{2.45}$$

The interactions between the graviton KK modes and the matter fields in the TeV brane can be derived from the 4-dimensional effective Lagrangian, once $h_{\mu\nu}$ is replaced by its KK decomposition:

$$\mathcal{L} = -\frac{1}{\overline{M}_{PL}} T^{\mu\nu}(x) h^{(0)}_{\mu\nu} - \frac{1}{e^{-kr_c\pi}\overline{M}_{PL}} T^{\mu\nu}(x) \sum_{n=1}^{\infty} h^{(n)}_{\mu\nu}(x); \tag{2.46}$$

$T^{\mu\nu}$ is the space energy-momentum tensor of the matter fields. The zero mode of the gravitons coupling is $1/\overline{M}_{PL}$, while higher order KK modes couplings to all SM fields are suppressed by $e^{-kr_c\pi}\overline{M}_{PL}$, that is of the order of the TeV scale. Spin-2 KK masses and couplings are hence determined by the TeV scale, or, equivalently, KK gravitons are close to the TeV brane. This implies that KK gravitons can be produced via $q\bar{q}$ or gluon fusion, and that a leptonic decay of the resonance could represent a very clear signal signature.

2.3.2 Bulk extension of RS1: graviton production and decays

An extension of the original RS1 formulation has been proposed. It states that the usual SM fields are no longer confined in the TeV brane, but they are the zero modes of the corresponding 5-dimensional SM fields. If first and second generation fermions are close to the Planck brane, contribution to flavour changing neutral currents by higher-dimensional operators are suppressed. These contributions are excluded by electroweak precision tests, but they were not prevented in original RS1. The second motivation behind the choice is, as mentioned previously, the naturally arising flavour hierarchy: first and second generation quarks have small Yukawa couplings to the Higgs sector, confined in the TeV brane, while top quark and bosons have stronger Yukawa couplings.
In this picture, couplings between higher-order KK gravitons and light fermions are strongly suppressed, resulting into a negligible KK gravitons production via $q\bar{q}$, whilst gluon fusion production becomes dominant. KK gravitons decay into top quarks and Higgs bosons are dominant, given that both their profiles are near the TeV brane, while leptonic decays are negligible. Via the equivalence theorem, the Goldstone bosons are equivalent to the longitudinally polarized weak bosons, $W_L^{\pm}$ and Z_L, that have profiles close to the TeV brane. Decays of KK gravitons into weak dibosons (and production in VBF) are comparable to di-top and di-Higgs decays.

The KK decomposition and the KK mass spectrum of the graviton have already been presented in sec. 2.3.1. The KK decomposition of a massless 5-dimensional gauge field $A_M(x,\phi)$ is similarly performed [35]:

$$A_\mu(x,\phi) = \sum_{n=0}^{\infty} A^{(n)}_\mu(x) \frac{\chi^{(n)_A}(\phi)}{\sqrt{r_c}}. \tag{2.47}$$

The profiles for the gauge fields are:

$$\chi^{(n)}_A(\phi) = \frac{e^\sigma}{N_A}\left[J_1(z^A_n) + \alpha^A_n Y_1(z^A_n)\right], \tag{2.48}$$

where J_1 and Y_1 are first order Bessel functions. Similarly to eq. 2.49, the mass spectrum of the gauge field is:

$$m^A_n = k z^A_n(\pi) e^{-kr_c\pi}; \tag{2.49}$$

the first roots of the Bessel functions are $z_n^A = (2.45, 5.57, 8.70, 11.84, ...)$.

The Lagrangian expressing the interaction between the m and n modes of the bulk field F to the q KK gravitons mode G is [35]:

$$\mathcal{L}_{G-F} = \sum_{m,n,q} C_{mnq}^{FFG} \frac{1}{\overline{M}_{PL}} \eta^{\mu\alpha}\eta^{\nu\beta} h_{\alpha\beta}^{(q)}(x) T_{\mu\nu}^{(m,n)}(x), \tag{2.50}$$

C_{mnq}^{FFG} is the overlap integral of the profiles:

$$C_{mnq}^{FFG} = \int \frac{d\phi}{\sqrt{k}} e^{t\sigma} \frac{\chi_F^{(m)}\chi_F^{(n)}\chi_G^{(q)}}{\sqrt{r_c}}; \tag{2.51}$$

t depends on the type of field considered.

The coupling between gluons and the q KK graviton mode is given by:

$$C_{00q}^{AAG} = e^{k\pi r_c} \frac{2\left[1 - J_0(x_n^G)\right]}{k\pi r_c (x_n^G)^2 \left|J_2(x_n^G)\right|}. \tag{2.52}$$

Once eq. 2.52 is put in eq. 2.50, the most significant partial decay widths into the q KK graviton mode are:

$$\begin{aligned}
\Gamma\left(G \to t_R \bar{t}_R\right) &\sim N_c \frac{\left[\tilde{k} x_q^G\right]^2 m_q^G}{320\pi} \\
\Gamma\left(G \to hh\right) &\sim \frac{\left[\tilde{k} x_q^G\right]^2 m_q^G}{960\pi} \\
\Gamma\left(G \to W_L^+ W_L^-\right) &\sim \frac{\left[\tilde{k} x_q^G\right]^2 m_q^G}{480\pi} \\
\Gamma\left(G \to Z_L Z_L\right) &\sim \frac{\left[\tilde{k} x_q^G\right]^2 m_q^G}{960\pi},
\end{aligned} \tag{2.53}$$

where $\tilde{k} = k/\overline{M}_{PL}$; the total decay width is:

$$\Gamma_G = \frac{13\left[\tilde{k} x_q^G\right]^2 m_q^G}{960\pi}. \tag{2.54}$$

Calculations, so far, have been performed considering $M \sim \overline{M}_{PL}$ and $k < M$, hypoteses under which the solution for the bulk metric (eq. 2.36) is valid. Hence, $\tilde{k} = k/\overline{M}_{PL} \leq 1$ is taken as a reference interval. This has also phenomenological consequences on the width of the resonance, as stated in eq. 2.54. The total decay width of the lightest KK graviton mode, compared to its mass, is shown as a function of $\tilde{k}$ in fig. 2.12 [36]. At $\tilde{k} = 1$, in the bulk scenario, the KK graviton width is expected to be few % of its mass, up to 4 TeV (dotted red curve). The narrow width approximation holds, hence the resonance properties can be probed at the peak, neglecting the effects in the tails of the mass distribution.

The total cross-section of a bulk graviton, produced at LHC in proton-proton interactions via gluon fusion (displayed in fig. 2.13), decaying into a couple of vector bosons (for the purpose of this thesis, a final state with two longitudinally polarized Z bosons is considered)

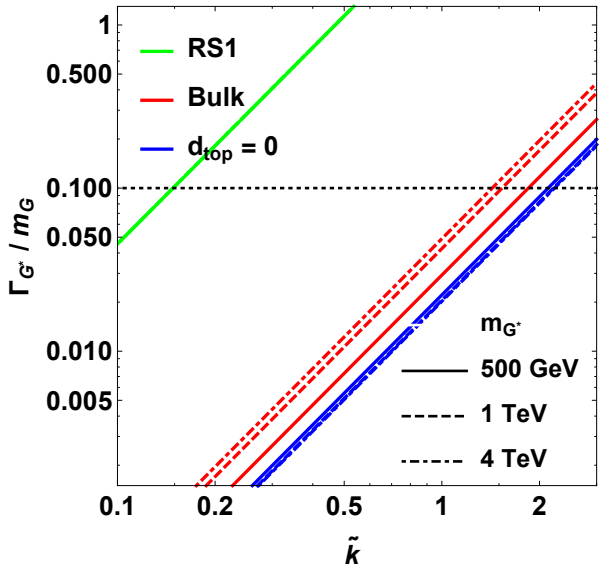

Figure 2.12: Width of the KK gravitons, in units of the mass of the resonance, as a function of the curvature parameter $\tilde{k}$. The red curves represent the bulk extension of RS1 original model for different mass hypoteses (from 500 GeV up to 4 TeV).

is expressed as a function of the parton level cross-section $\hat{\sigma}$, the gluon parton distribution functions f_q, the momentum transfer $Q^2 \sim (m_q^G)^2$ and the center-of-mass energy s:

$$\sigma(pp \to ZZ) = \int dx_1 dx_2 f_g(x_1, Q^2) f_g(x_2, Q^2) \hat{\sigma}(x_1 x_2 s). \tag{2.55}$$

The differential parton level cross-section, averaged over colors and initial spin states, is (hatted quantities are calculated in the center-of-mass frame):

$$\frac{d\hat{\sigma}(gg \to ZZ)}{d\cos\hat{\theta}} \approx \frac{|\mathcal{M}_{+-00}|^2}{1024\pi\hat{s}}, \tag{2.56}$$

where $|\mathcal{M}_{+-00}|$ is the matrix element of the dominant contribution in $gg \to VV$ process (Γ_G is defined in eq. 2.54, a, b are color factors):

$$\mathcal{M}_{+-00}(g^a g^b \to VV) = -C_{00q}^{AAG} e^{-k\pi r_c} \left(\frac{x_n^G \tilde{k}}{m_n^G}\right)^2 \sum_n \frac{\delta_{ab}\mathcal{A}_{+-00}}{\hat{s} - m_n^{G\,2} + i\Gamma_G m_n^G}. \tag{2.57}$$

The relevant amplitudes taken account in the matrix element calculation are [31]:

$$\mathcal{A}_{+-00} = \mathcal{A}_{-+00} = \frac{\left(1 - 1/\beta_Z^2\right)\left(\beta_Z^2 - 2\right)\left[(\hat{t} - \hat{u})^2 - \beta_Z^2 \hat{s}^2\right]\hat{s}}{8M_Z^2}, \tag{2.58}$$

where $\beta_Z^2 = 1 - 4M_Z^2/\hat{s}$ and M_Z is the mass of the Z boson.

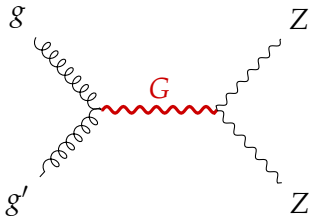

Figure 2.13: Gluon fusion production mechanism for a KK graviton that decays in a couple of Z bosons.

2.3.3 Search for KK bulk gravitons at LHC

No evidence of spin-2 bulk graviton resonances has been observed so far at LHC experiments. Data collected by ATLAS and CMS detectors are used to set limits on the graviton masses, generally considering different curvature parameter $\tilde{k}$ hypoteses, once assured the narrow width approximation is still valid (up to $\tilde{k} \sim 1$). The most stringent limits have been set with Run 2 data.

Many results of the diboson searches performed at CMS and already presented in sec. 2.2.6 are interpreted in the context of the bulk gravitons, together with the additional final states $WZ, ZZ \to \ell\bar{\ell}\nu\bar{\nu}$ [37] and $HH \to b\bar{b}b\bar{b}$ [38]. The most interesting limit is provided by [37], that, under the hypotesis $\tilde{k} = 0.5$, excludes a spin-2 bulk graviton with a mass lower than 800 GeV (fig. 2.14).

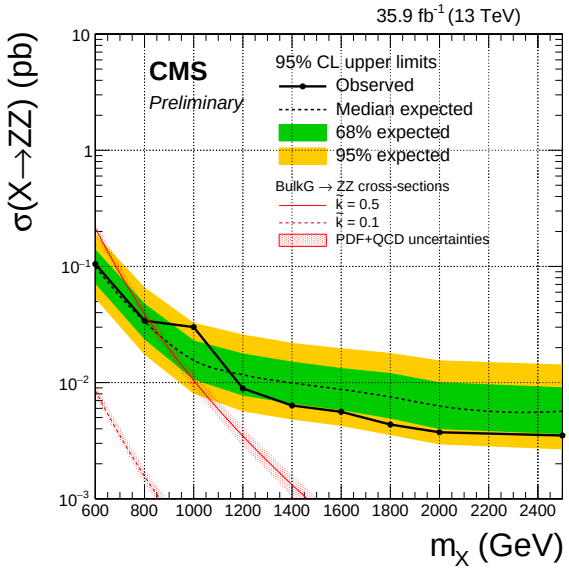

Figure 2.14: The observed and expected limits, with 68% and 95% uncertainty bands, on the product of the cross section and branching fraction $\sigma\mathcal{B}(G \to ZZ)$ for a spin-2 bulk graviton, as a function of the reconstructed mass of the diboson resonance. The colored lines show the theoretical predictions for $\tilde{k} = 0.1$ and 0.5.

Similarly for ATLAS experiment, searches for diboson resonances in sec. 2.2.6 have been

interpreted in the graviton context. The most stringent limit is given by [25], where, under the assumption $\tilde{k} = 1$, a spin-2 bulk graviton with mass lower than 1.76 TeV is excluded (fig. 2.15).

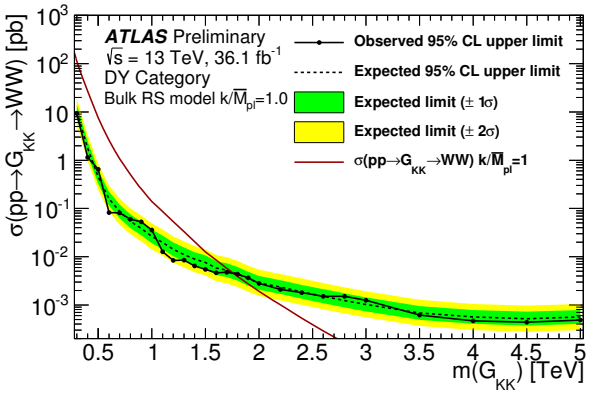

Figure 2.15: The observed and expected limits, with 68% and 95% uncertainty bands, on the product of the cross section and branching fraction $\sigma\mathcal{B}(G \to ZZ)$ for a spin-2 bulk graviton, as a function of the reconstructed mass of the diboson resonance. The colored lines show the theoretical predictions for $\tilde{k} = 1$.

Chapter 3

The Large Hadron Collider and the CMS experiment

Meh

Chapter 4

Data and Monte Carlo samples

Chapter 5

Physics objects

Chapter 6

Diboson candidate reconstruction

Chapter 7

Background estimation

Chapter 8

Systematic uncertainties

Chapter 9

Results

Chapter 10

Conclusions

Bibliography

[1] G. Aad *et al.*, "Observation of a new particle in the search for the Standard Model Higgs boson with the ATLAS detector at the LHC," *Phys. Lett. B*, vol. 716, p. 1, 2012.

[2] S. Chatrchyan *et al.*, "Observation of a new boson at a mass of 125 GeV with the CMS experiment at the LHC," *Phys. Lett. B*, vol. 716, p. 30, 2012.

[3] S. Chatrchyan *et al.*, "Observation of a new boson with mass near 125 GeV in pp collisions at $\sqrt{s}$ = 7 and 8 TeV," *JHEP*, vol. 06, p. 081, 2013.

[4] G. Aad *et al.*, "Evidence for the spin-0 nature of the Higgs boson using ATLAS data," *Phys. Lett. B*, vol. 726, p. 120, 2013.

[5] V. Khachatryan *et al.*, "Precise determination of the mass of the Higgs boson and tests of compatibility of its couplings with the standard model predictions using proton collisions at 7 and 8 TeV," *Eur. Phys. J. C*, vol. 75, p. 212, 2015.

[6] G. Aad *et al.*, "Measurement of the Higgs boson mass from the $H \to \gamma\gamma$ and $H \to ZZ^* \to 4\ell$ channels in pp collisions at center-of-mass energies of 7 and 8 TeV with the ATLAS detector," *Phys. Rev. D*, vol. 90, p. 052004, 2014.

[7] CMS and ATLAS Collaborations, "Combined Measurement of the Higgs Boson Mass in pp Collisions at $\sqrt{s} = 7$ and 8 TeV with the ATLAS and CMS Experiments." Submitted to Phys. Rev. Lett., 2015.

[8] G. Degrassi, S. Di Vita, J. Elias-Miro, J. R. Espinosa, G. F. Giudice, G. Isidori, and A. Strumia, "Higgs mass and vacuum stability in the Standard Model at NNLO," *JHEP*, vol. 08, p. 098, 2012.

[9] D. Pappadopulo, A. Thamm, R. Torre, and A. Wulzer, "Heavy vector triplets: bridging theory and data," *Journal of High Energy Physics*, vol. 2014, no. 9, pp. 1–50, 2014.

[10] V. D. Barger, W.-Y. Keung, and E. Ma, "A Gauge Model With Light W and Z Bosons," *Phys. Rev.*, vol. D22, p. 727, 1980.

[11] C. Grojean, E. Salvioni, and R. Torre, "A weakly constrained W' at the early LHC," *JHEP*, vol. 07, p. 002, 2011.

[12] R. Contino, D. Pappadopulo, D. Marzocca, and R. Rattazzi, "On the effect of resonances in composite higgs phenomenology," *Journal of High Energy Physics*, vol. 2011, no. 10, pp. 1–50, 2011.

[13] B. Bellazzini, C. Csáki, and J. Serra, "Composite Higgses," *Eur. Phys. J.*, vol. C74, no. 5, p. 2766, 2014.

[14] G. F. Giudice, C. Grojean, A. Pomarol, and R. Rattazzi, "The Strongly-Interacting Light Higgs," *JHEP*, vol. 06, p. 045, 2007.

[15] A. Wulzer, "An Equivalent Gauge and the Equivalence Theorem," *Nucl. Phys.*, vol. B885, pp. 97–126, 2014.

[16] A. M. Sirunyan *et al.*, "Search for massive resonances decaying into WW, WZ, ZZ, qW, and qZ with dijet final states at sqrt(s) = 13 TeV," 2017.

[17] CMS Collaboration, "Search for massive resonances decaying into WW, WZ, ZZ, qW and qZ in the dijet final state at $\sqrt{s} = 13$ TeV," CMS Physics Analysis Summary CMS-PAS-B2G-17-001, CERN, Geneva, 2017.

[18] C. Collaboration, "Search for heavy resonances decaying into a vector boson and a Higgs boson in hadronic final states with 2016 data," 2017.

[19] CMS Collaboration, "Search for heavy resonances decaying into a vector boson and a Higgs boson in hadronic final states with 2016 data," CMS Physics Analysis Summary CMS-PAS-B2G-17-002, CERN, Geneva, 2017.

[20] CMS Collaboration, "Search for heavy resonances decaying into a Z boson and a W boson in the $\ell^+\ell^-\mathrm{q\bar{q}}$ final state," CMS Physics Analysis Summary CMS-PAS-B2G-16-022, CERN, Geneva, 2017.

[21] V. Khachatryan *et al.*, "Search for heavy resonances decaying into a vector boson and a Higgs boson in final states with charged leptons, neutrinos, and b quarks," *Phys. Lett.*, vol. B768, pp. 137–162, 2017.

[22] CMS Collaboration, "Search for new resonances decaying to WW/WZ $\rightarrow \ell\nu$qq," CMS Physics Analysis Summary CMS-PAS-B2G-16-020, CERN, Geneva, 2016.

[23] CMS Collaboration, "Search for heavy resonances decaying into a Z boson and a vector boson in the $\nu\nu\ q\bar{q}$ final state," CMS Physics Analysis Summary CMS-PAS-B2G-17-005, CERN, Geneva, 2017.

[24] M. Aaboud *et al.*, "Search for diboson resonances with boson-tagged jets in pp collisions at $\sqrt{s} = 13$ TeV with the ATLAS detector," 2017.

[25] ATLAS Collaboration, "Search for WW/WZ resonance production in $\ell\nu qq$ final states in pp collisions at $\sqrt{s}$ = 13 TeV with the ATLAS detector," ATLAS Conference Note ATLAS-CONF-2017-051, CERN, Geneva, Jul 2017.

[26] "Searches for heavy ZZ and ZW resonances in the llqq and vvqq final states in pp collisions at sqrt(s) = 13 TeV with the ATLAS detector," ATLAS Conference Note ATLAS-CONF-2016-082, CERN, Geneva, Aug 2016.

[27] M. Aaboud *et al.*, "Search for heavy resonances decaying to a W or Z boson and a Higgs boson in the $q\bar{q}^{(\prime)}b\bar{b}$ final state in pp collisions at $\sqrt{s} = 13$ TeV with the ATLAS detector," 2017.

[28] ATLAS Collaboration, "Search for heavy resonances decaying to a W or Z boson and a Higgs boson in final states with leptons and b-jets in 36.1 fb^{-1} of pp collision data at $\sqrt{s} = 13$ TeV with the ATLAS detector," ATLAS Conference Note ATLAS-CONF-2017-055, CERN, Geneva, Jul 2017.

[29] L. Randall and R. Sundrum, "A Large mass hierarchy from a small extra dimension," *Phys. Rev. Lett.*, vol. 83, pp. 3370–3373, 1999.

[30] L. Randall and R. Sundrum, "An Alternative to compactification," *Phys. Rev. Lett.*, vol. 83, pp. 4690–4693, 1999.

[31] K. Agashe, H. Davoudiasl, G. Perez, and A. Soni, "Warped Gravitons at the LHC and Beyond," *Phys. Rev.*, vol. D76, p. 036006, 2007.

[32] A. L. Fitzpatrick, J. Kaplan, L. Randall, and L.-T. Wang, "Searching for the Kaluza-Klein Graviton in Bulk RS Models," *JHEP*, vol. 09, p. 013, 2007.

[33] H. Davoudiasl, J. L. Hewett, and T. G. Rizzo, "Phenomenology of the Randall-Sundrum Gauge Hierarchy Model," *Phys. Rev. Lett.*, vol. 84, p. 2080, 2000.

[34] T. Gherghetta and A. Pomarol, "Bulk fields and supersymmetry in a slice of AdS," *Nucl. Phys.*, vol. B586, pp. 141–162, 2000.

[35] H. Davoudiasl, J. L. Hewett, and T. G. Rizzo, "Experimental probes of localized gravity: On and off the wall," *Phys. Rev.*, vol. D63, p. 075004, 2001.

[36] A. Oliveira, "Gravity particles from Warped Extra Dimensions, predictions for LHC," 2014.

[37] CMS Collaboration, "Search for diboson resonances in the $2l2\nu$ final state," CMS Physics Analysis Summary CMS-PAS-B2G-16-023, CERN, Geneva, 2017.

[38] CMS Collaboration, "Search for heavy resonances decaying to a pair of Higgs bosons in the four b quark final state in proton-proton collisions at $\sqrt{s} = 13$ TeV," CMS Physics Analysis Summary CMS-PAS-B2G-16-026, CERN, Geneva, 2017.